Supplementary Material

Figure S1. A specific interaction between the mSin3A PAH1 domain and the SAP25 SID. (**a**) The ^{1}H-^{15}N correlated NMR spectrum of the apo-mSin3A PAH1 domain recorded at 15 °C. (**b**) The corresponding spectrum recorded in the presence of one equivalent of SAP25 SID at 30 °C. The horizontal lines connect side chain amide correlations of glutamines and asparagines. Residue-specific backbone and side chain assignments are indicated in blue and magenta, respectively. Arginine side chain resonances are distinguished by colored ovals. Residues of the PAH1 domain that exhibit resonance line broadening in the complex are italicized and underlined. Minor peaks arising from incomplete cyclization of the N-terminal glutamine residue (Gln119) are denoted by asterisks.

Figure S2. A specific, high-affinity interaction between SAP25 SID and mSin3A PAH1 domain. (**a**) ^{1}H-^{15}N correlated spectrum of apo-SAP25 SID recorded at 30 °C. (**b**) An overlay of the ^{1}H-^{15}N correlated spectra of SAP25 SID in the apo (black) and PAH1-bound (red) states recorded under the same conditions. Sequence-specific resonance assignments for the SAP25 segment spanning Thr128–Thr150 that is most strongly affected by complex formation are shown. The complex is in slow exchange on the NMR timescale as evidenced by the disappearance of resonances within this segment belonging to the free form and the concomitant appearance at a different location corresponding to the bound form upon titrating with increasing amounts of PAH1. The enhanced dispersion of SAP25 amide proton resonances in the PAH1-bound form is readily evident.

Figure S3. Quantitative analysis of SID–PAH interactions. (**a**) ITC binding isotherms resulting from titrations of mSin3A PAH1 with SAP25 SID. The starting concentrations of the SAP25 SID peptide (in the cell) and mSin3A PAH1 (in the syringe) were 20 μM and 1.0 mM, respectively. The experimental data are presented as filled symbols while the solid line is the curve resulting from the non-linear least-squares fitting procedure assuming a single binding-site model (*bottom panel*; fitted values: K_d = 134 nM; ΔH_a = –9.96 kcal mol^{-1}; n = 1.36). (**b**) Representative fluorescence anisotropy binding isotherms resulting from titrations of GST-tagged wild-type and mSin3A PAH2 mutant proteins with a fluoresceinated Mad1/Mxd1 SID peptide. The experimental data are presented as filled symbols while the solid lines are the

curves resulting from the non-linear least-squares fitting procedure. The reported anisotropy values are the average and standard deviations from three independent samples. The fitted values are presented in Table 2.

Figure S4. The mSin3A PAH1 and the SAP25 SID domains undergo mutually coupled conformational changes upon complex formation. (**a**) Atomic root-mean-square deviations of backbone atoms following a best-fit superposition of the ordered regions in the apo- and SAP25 SID-bound states of mSin3A PAH1 graphed as a function of residue number. (**b**) Secondary $^{13}C^{\alpha}$ chemical shifts of the apo (purple) and mSin3A PAH1-bound (black) states of SAP25 SID. The cartoons on top of each graph identify the locations of the helices in the respective proteins in the complex.

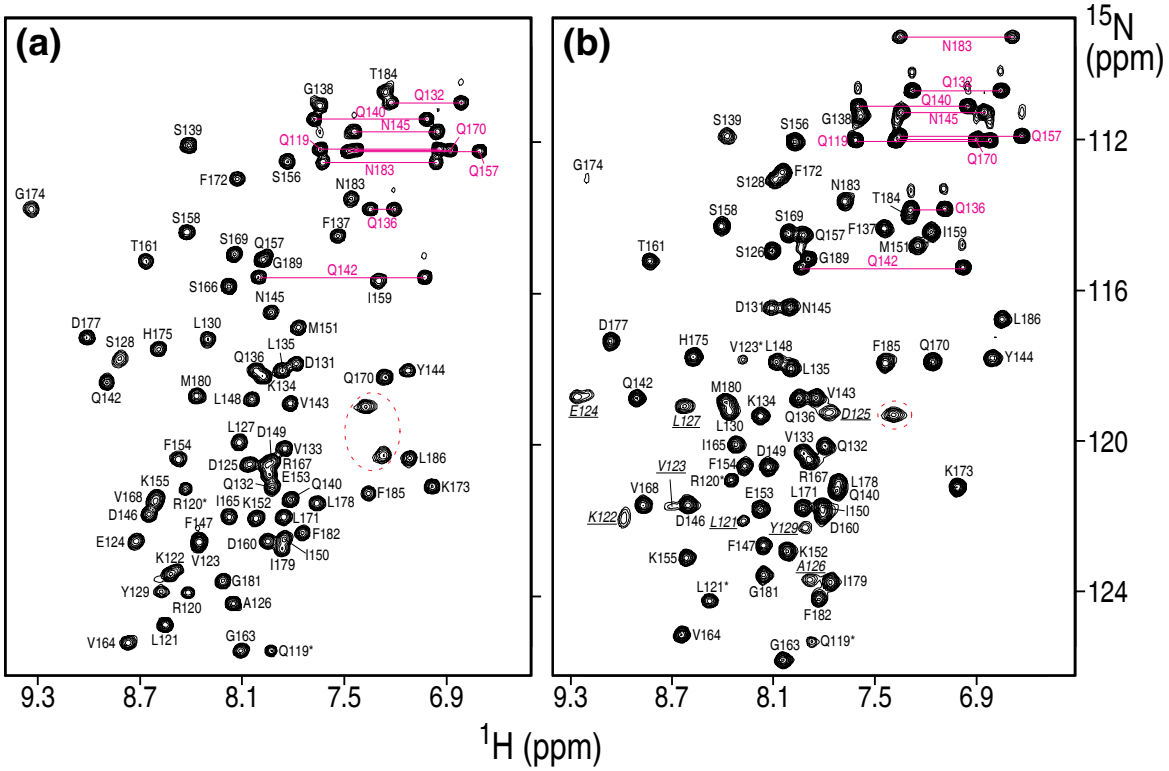

Supplementary Figure S1

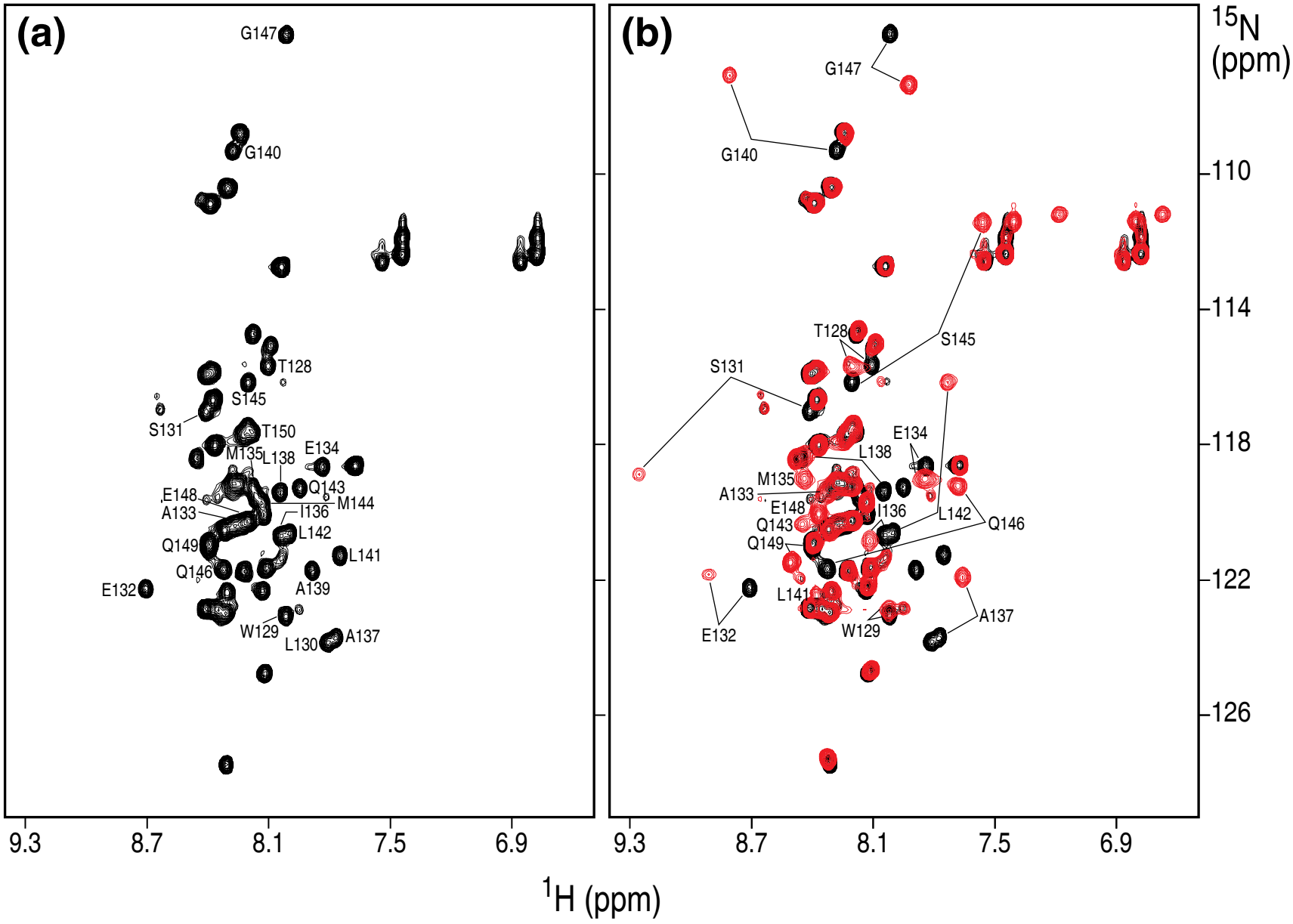

Supplementary Figure S2

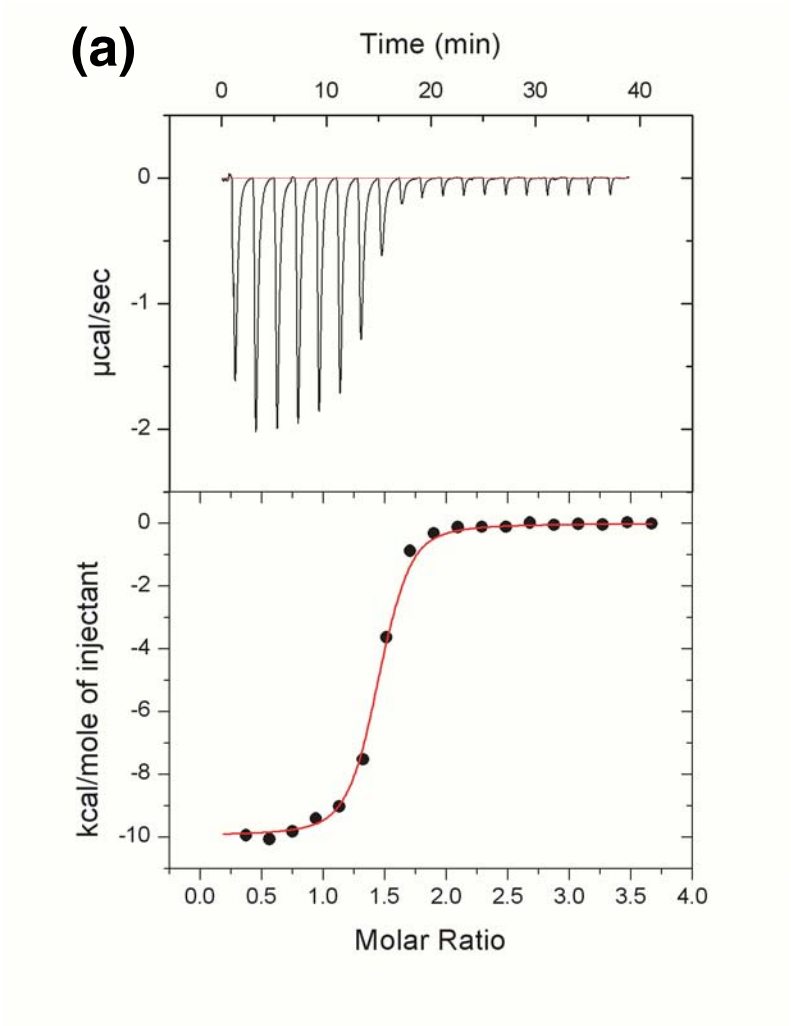

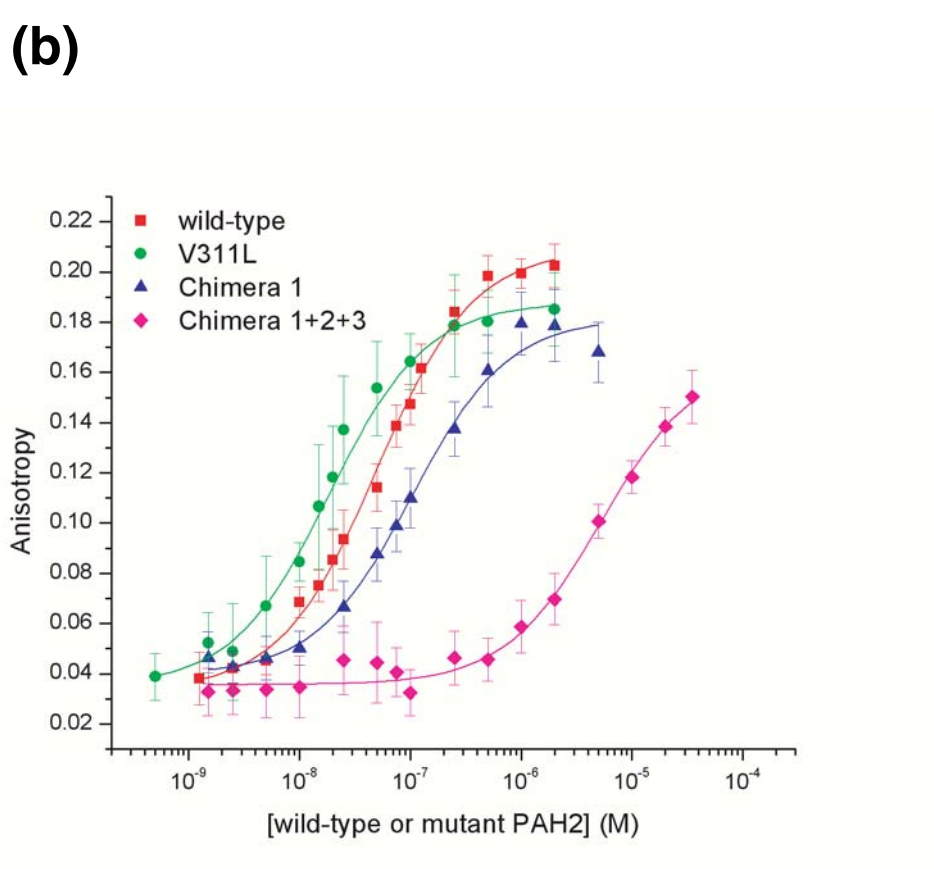

Supplementary Figure S3

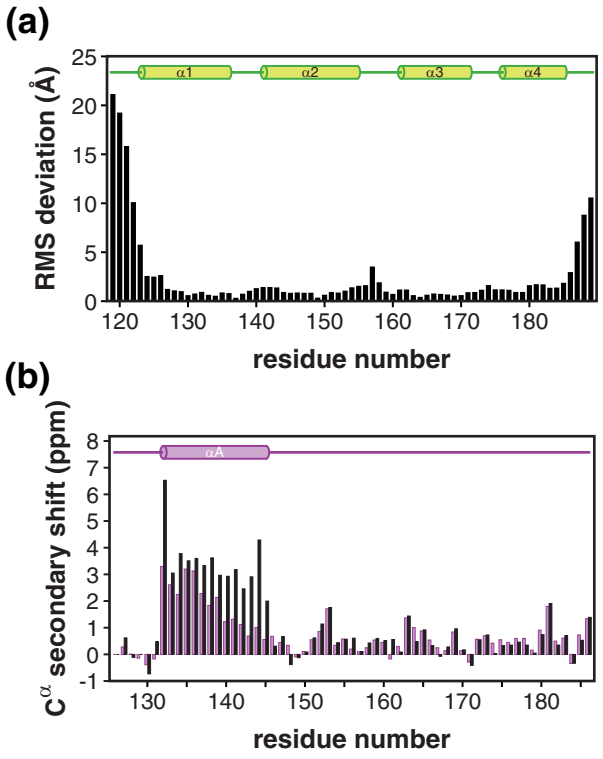

Supplementary Figure S4